Institute for Energy

SENSITIVITY OF RISK REDUCTION TO PROBABILITY OF DETECTION CURVES (POD) LEVEL AND DETAIL

Authors: Luca Gandossi, Kaisa Simola

DG JRC
Institute for Energy
2007

JRC
EUROPEAN COMMISSION
EUR 21902 EN

Mission of the Institute for Energy
The Institute for Energy provides scientific and technical support for the conception, development, implementation and monitoring of Community policies related to energy. Special emphasis is given to the security of energy supply and to sustainable and safe energy production.

European Commission
Directorate-General Joint Research Centre (DG JRC)
http://www.jrc.ec.europa.eu/

Institute for Energy, Petten (the Netherlands)
http://ie.jrc.ec.europa.eu/

Contact details:
Luca Gandossi
Tel: +31 (0)224 56 5250
E-mail: luca.gandossi@jrc.nl

EUR 21902 EN
ISSN 1018-5593
Luxembourg: Office for Official Publications of the European Communities

Printed in the Netherlands

SENSITIVITY OF RISK REDUCTION TO PROBABILITY OF DETECTION CURVES (POD) LEVEL AND DETAIL

Luca Gandossi & Kaisa Simola

May 2007

FOREWORD

The output from the European inspection qualification process is generally a statement concluding whether or not there is high confidence that the required inspection capability will be achieved in practice, for the specified inspection system, component and defect range. However, this process does not provide a quantitative measure of inspection capability of the type that could be used for instance in the connection of the risk-informed in-service inspection (RI-ISI) process. In a quantitative RI-ISI, a quantitative measure of inspection effectiveness is needed in determining the risk reduction associated with inspection.

The issue of linking the European qualification process and a quantitative measure of inspection capability has been discusses within the ENIQ (European Network for Inspection and Qualification) over several years. In 2005 the ENIQ Task Group on Risk decided to initiate an activity to address this question. A program of work was proposed to investigate and demonstrate an approach to providing some objective measure of the confidence which comes from inspection qualification, and allowing risk reduction associated with a qualified inspection to be calculated. The work plan focuses on following issues:

- Investigating sensitivity of risk reduction to POD level and detail;
- Investigating the use of user-defined POD curve as target for qualification;
- Testing a Bayesian approach to quantifying output from qualification;
- Linking qualification outcome, risk reduction and inspection interval;
- Pilot study of overall process, including a pilot qualification board.

The work is organised in a project “Link Between Risk-Informed In-Service Inspection and Inspection Qualification”, coordinated by Doosan Babcock, UK. The project is partly funded by a group of nuclear utilities. In addition, the Joint Research Centre, Institute of Energy is participating in the project with a significant work contribution.

This report contributes to the project by addressing the investigation of the sensitivity of risk reduction POD level and detail. The research work has been carried out at the Joint Research Centre, Institute for Energy during year 2006.

Luca Gandossi
Scientific Officer
DG Joint Research Centre (JRC-IE)

Kaisa Simola
Senior Research Scientist
VTT Technical Research Centre of Finland
(Visiting Scientist at JRC-IE 2004-2006)

1 Introduction

This report discusses the link between risk-informed in-service inspection (RI-ISI) and assumptions made concerning the probability of flaw detection. The purpose is to investigate the reasonable and practical requirements that should be set for assumptions about the accuracy of probability of detection (POD) curves from a RI-ISI point of view.

RI-ISI aims at defining an effective inspection programme taking into account the probability of failure and the failure consequences. When evaluating the effectiveness of a RI-ISI programme, a measure of the inspection reliability is needed. The change in risk is affected by the assumptions made on the inspection efficiency. A basic assumption is that an inspection decreases the failure probability of the inspected component, and thus reduces the risk associated with that component.

An acceptance criterion for a new inspection programme based on a RI-ISI analysis is typically that the safety level of the plant should be maintained or improved when moving from a traditional inspection programme to a risk-informed one. In some cases a minor risk increase may be acceptable, as in the US Nuclear Regulatory Commission regulation [1, 2]. Requirements may also be set for the risk reduction when the situation with no inspections at all is compared with the risk calculated accounting for the inspections.

In various RI-ISI methodologies, the inspection reliability is taken into account in different ways. In the EPRI methodology, a very simple approach of using a single POD value to reduce the failure probability is adopted for evaluating the risk change. In the Swedish NURBIT code [3], full POD curves where the POD is a function of the flaw through-wall extent are used. The POD function can either be determined by the user or built-in functions based on the study of [4] can be selected. Also some other structural reliability models use rather detailed POD models.

Even if the use of a single POD value seems to be a very coarse approach, one may also question the use of very detailed models, since the validity of the applied POD curves can easily be questioned. This report aims at studying the sensitivity of the risk reduction to the assumptions made about the POD function. A reasonable level of detail for a POD (at least for RI-ISI applications) might be to express it as a step function, and we have investigated especially the effect of the step function parameters on the risk reduction. The results of these sensitivity studies can be used to develop recommendations for a reasonable degree of detail for PODs.

2 A simplified model for considering inspection reliability in RI-ISI

As a starting point, let us set out the framework of this analysis. We consider passive pressure-retaining components, such as pipework and pressure vessels. We deal with the problem of inspecting such components (or selected parts of them, such as weldments, elbows, tees) with the specific aim of finding (or excluding the presence of) crack-like defects. We assume that we are dealing with a single degradation mechanism (i.e. fatigue, or intergranular stress corrosion cracking) and we exclude from our analysis degradation leading to volumetric defects, wall thinning, etc.

We start with the analysis of a single component (for instance, one weld in a piping system).

This component has an associated risk which is typically calculated as the product of the probability of failure and the consequence of failure. We limit our analysis to a failure that could occur because of the (possible) presence of a crack-like defect as specified above.

In broad engineering terms, the risk is given by

$$\text{Risk}=pof \times cof \tag{1}$$

where *pof* is the probability of failure and *cof* the consequence of that failure, expressed in some sort of convenient metric.

Clearly, this is not the only risk that could be associated with that single component. The component (along with all other components constituting the plant) will carry a total risk given by the sum of the risks associated with all other relevant degradation mechanisms, say for instance water hammer, wall thinning due to corrosion and earthquake. We assume that the inspection system under consideration has been designed to target the specific acting degradation mechanism leading to crack-like defects. In this framework, the inspection programme and the detection capabilities of the inspection system will not affect any other components of the risk except that expressed in Equation (1).

Further, it is clear to see that the inspection programme will only affect the probability of failure. As an inspection is carried out, some knowledge regarding the (previously uncertain) state of the plant is gathered, and the probability of failure is (usually) reduced. If defective components are found, these are assumed to be repaired or removed. The consequence of failure, depending on many factors such as plant layout, presence of redundant or mitigating systems, etc. will not be affected by the inspection. It is therefore straightforward to see how the risk will change before and after an inspection is carried out by simply considering the change in probability of failure.

Let us define a risk reduction percentage, *R*, as:

$$R = \left(1 - \frac{pof_{with}}{pof_{without}}\right) \cdot 100 \tag{2}$$

where $pof_{without}$ is the probability of failure without inspection, and pof_{with} is the probability of failure with inspection. *R* takes values in the interval (0,100). Values of *R* close to 100 mean a significant risk reduction due to the inspection. Indeed, a perfect inspection (i.e. one capable of finding all defects of all sizes) will reduce the probability of failure pof_{with} to zero, and therefore *R* will be equal to 100. On the other hand, values of *R* close to zero mean a small change in risk, due to a poor inspection.

In a detailed, fully quantitative approach to RI-ISI, one would model the inspection programme within a probabilistic structural integrity model. In this case, extensive knowledge or assumptions are needed about materials, loadings, initial crack distribution, crack growth behaviour, probability of detection, etc. Typically, one would run a MONTECARLO analysis of the problem, repeating many times over a deterministic structural integrity assessment, each time sampling the required input

parameters from the appropriate distributions and verifying whether the structure has failed or is in a safe state for that particular combination of input variables. Such probabilistic analysis, explicitly taking into account the uncertainties associated with the input parameters, can offer a much better picture than a simple deterministic calculation. The main drawback is the much higher requirement in terms of resources such as time, calculating power, need to know (or to make assumptions about) material properties, loadings, etc.

We here consider a simplified approach. Let us, for the time being, ignore the possibility of any crack development (growth).

Let us postulate the presence of an inner surface breaking crack in the component at hand. The through-wall extent of such crack, a, (also called “depth” in the remainder of this report) is assumed to be the random variable. We use a non-dimensional measure of the crack depth, normalising the true depth to the component thickness. Therefore, *a* takes values in the interval (0, 1).

Let us consider the following functions:

- A probability distribution of flaw size, $\lambda(a)$
- A function expressing the probability of failure as a function of flaw size, $\phi(a)$
- A POD curve, $p(a)$

As the nomenclature can be confusing, it is important to note that whereas $\lambda(a)$ is a true probability density function, $\phi(a)$ and $p(a)$ are not.

If the functions $\lambda(a)$, $\phi(a)$ and $p(a)$ are defined, it is straightforward to calculate the probability of failure without inspection, $pof_{without}$, by integrating $\lambda(a) \times \phi(a)$ over the flaw size:

$$pof_{without} = \int_0^1 \lambda(a)\phi(a)da \tag{3}$$

And, since 1-$p(a)$ is the probability of missing a defect of size *a*, the probability of failure with inspection, pof_{with}, is given by:

$$pof_{with} = \int_0^1 \lambda(a)\phi(a)(1-p(a))da \tag{4}$$

Thus, the risk reduction percentage expressed in Equation 2 can be easily evaluated. In the following, we will use this quantity to investigate the effects of employing different POD curves p(a).

It is important to point out the fact that the number (or frequency) of cracks has no real relevance in this investigation, since it would increase pof_{with} by the same percentage as $pof_{without}$, and *R* would remain unchanged.

In our approach, we assume that the probability of failure, $\phi(a)$, and the probability of detection, $p(a)$, are functions of crack depth only. In reality, the probability of failure could well be dependent on crack length and other parameters, and the probability of detection (depending on the NDT system under consideration) would most certainly

also depend on factors such as crack length, tilt, skew, as well as weld geometry, etc. On the other hand, it is common practice – because of great analytical simplification – to express the problem as a function of one parameter only, with crack depth *a* usually being the most significant one.

3 Choice of input functions

As we have seen, in our simplified model, three input functions are required. The probability of detection curve, p(a), can be seen as "controlled" by the user. On the other hand, $\lambda(a)$ and $\phi(a)$ should be representative of the situation at hand.

3.1 Flaw depth distribution, $\lambda(a)$

$\lambda(a)$ should represent the true crack depth distribution for the type of component and acting damage mechanism. A common lack of real plant data (cracks are usually extremely infrequent in nuclear piping) makes the choice of the appropriate distribution a rather difficult task. It would actually be very difficult to determine which distribution could appropriately model a defect population even in the case of more frequent defects.

In this report, we will perform some analyses using the truncated exponential distribution. This is convenient for several reasons. First of all, the limited experience available [5, 6] has shown that the depth of real cracks can be modelled with an exponential distribution. Secondly, the distribution is defined by a single parameter (mathematically convenient) and it is proper in the interval [0,1] (i.e. the integral of the function over the interval is always equal to 1, regardless of the value taken by the parameter, and thus the probability distribution does not "predict" cracks that are longer than the thickness). Thirdly, the uniform distribution can be obtained as a special case.

A truncated exponential distribution is defined by the equation below

$$\begin{aligned} f(x) &= \frac{1}{\mu}\cdot e^{-\frac{1}{\mu}x}\cdot\frac{1}{1-e^{-\frac{1}{\mu}a_{\max}}} && 0\le x\le a_{\max} \\ f(x) &= 0 && x > a_{\max} \end{aligned} \tag{5}$$

where μ is the expected value of the associated (non-truncated) exponential distribution, and a_{max} defines the limit of the truncation. The expected value is given by:

$$E(x) = \mu - a_{\max}\cdot\frac{e^{-\frac{1}{\mu}a_{\max}}}{1-e^{-\frac{1}{\mu}a_{\max}}} \tag{6}$$

In our case, a_{max}=1. The uniform distribution can be obtained for $\mu\to\infty$, in which case E(x)=1/2.

In Figure 1 are plotted some distributions obtained for different values of μ. In a realistic situation, we would expect the defect depth distribution to be represented by curves

similar to the first 2 plotted in the Figure (μ=0.01 and μ=0.1). Using values of μ greater than this would seem overly conservative, but we will nonetheless also investigate the limiting case of $\mu \to \infty$, representing a uniform distribution of crack depths over the component thickness.

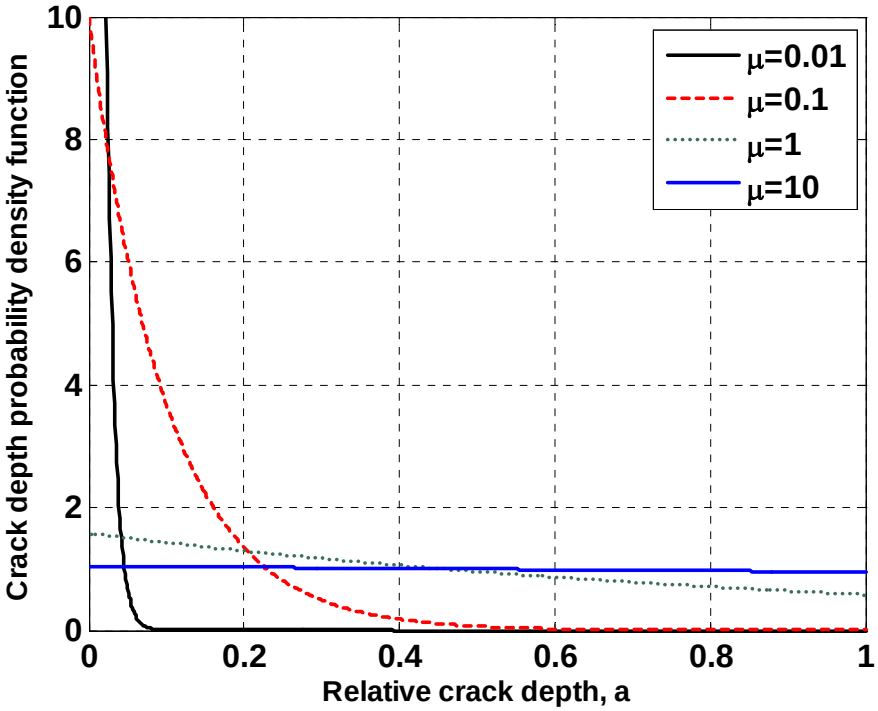

Figure 1 Truncated exponential distributions (equation 5, with a_{max}=1)

3.2 Probability of failure as a function of flaw size, $\phi(a)$

The function $\phi(a)$ expresses the probability of failure given that a crack of size *a* is present. It is, implicitly, a function of the material properties, the applied loading and the failure criteria that apply to the situation at hand.

Firstly, we assume that $\phi(a)$=0 for a=0 (quite reasonably, the probability of failure for a crack whose size is 0 must be zero) and that $\phi(a)$=1 for a=1 (i.e. a failure of the component is assumed if the crack becomes fully penetrating, again a rather reasonable assumption although this excludes the possibility of leak-before-break considerations).

For modelling convenience, we choose to represent $\phi(a)$ with the cumulative Beta distribution.

The probability density function (pdf) of the distribution is defined on the interval [0, 1]:

$$f(x;\alpha,\beta) = \frac{1}{B(\alpha,\beta)}(1-x)^{\beta-1}x^{\alpha-1} \qquad (7)$$

where $B(x,y)$ is the Beta function:

$$B(x,y)=\int_0^1 t^{x-1}(1-t)^{y-1}dt \tag{8}$$

The cumulative Beta distribution function, F(x;α,β) is thus defined as:

$$F(x;\alpha,\beta)=\int_0^x f(t;\alpha,\beta)dt \tag{9}$$

We choose to represent $\phi(a)$ with a cumulative Beta distribution function:

$$\phi(x;\alpha,\beta)=F(x;\alpha,\beta) \tag{10}$$

Changing the two parameters α and β allows us to obtain several different shapes that could conveniently represent different situations (in a simplified way). In Figure 2, three curves obtained using Equation 9 are plotted. The first one (solid line) is obtained for α=1 and β=1 and represents a situation in which the probability of failure is directly proportional to the flaw depth. The second one (dashed line) is obtained for α=100 and β=10 and represents a situation where the probability of failure is very low (virtually zero) for crack sizes up to approximately a=0.8, then "jumps" quickly to 1. This could be representative of a component which is very tolerant to the presence of crack-like defects, for instance because the material toughness is high. The third curve (dotted line) is obtained for α=10 and β=100, thus representing the opposite situation of a component not very tolerant to the presence of crack-like defects, for instance because the material toughness is low or because of the nature of the applied through-wall loading.

See Appendix 1 for an example of how this simplified model can fit a real structural integrity problem.

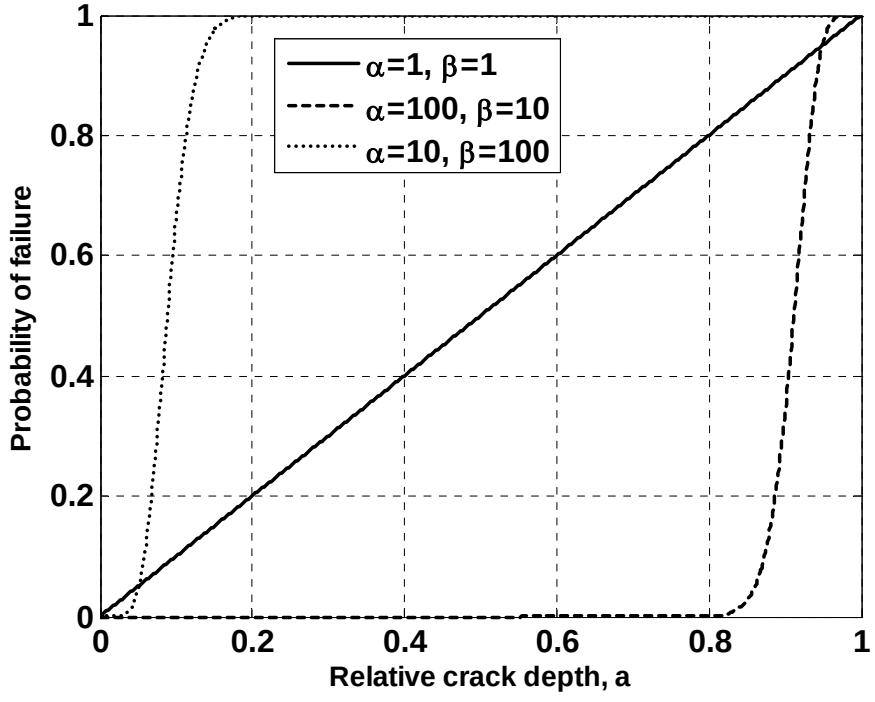

Figure 2 Curves representing possible shapes of the function $\phi(a)$

3.3 Probability of detection curve, *p(a)*

The POD curve, *p(a)*, expresses the probability that a defect of given size *a* will be found by the inspection system. Expressing in this way the reliability of the inspection system is a convenient simplification for the present purposes, but it must be recognised that there are several other factors that in general will affect the probability of detection of a defect, such as defect length, tilt, skew, etc. A probability of detection curve is often represented as a monotonically increasing function of crack size [7], starting from *p(a=0)=0* and rising more or less sharply to reach a plateau for crack depths larger than a certain value. Even if such behaviour seems intuitive (and it may be strictly true for some ultrasonic techniques, for instance the inspection of small smooth planar defects at normal angles, when the signal reflected by the crack is proportional to the crack area), it is important to be careful about this assumption. Other techniques, such as time-of-flight diffraction (TOFD) or the inspection of misoriented smooth cracks with conventional pulse-echo probes, rely on the identification of the crack edge. In such cases, a probability of detection curve plotted against crack depth could even show a decrease for larger cracks.

In this study, we will investigate user-defined POD curves. A first convenient approximation is to suppose that the POD is zero for all crack sizes *a* below a certain threshold depth a_{th}, and equal to a plateau value p_{pl} for $a > a_{th}$. In Figure 3, two such curves are illustrated, the first defined for a_{th}=0.2 and p_{pl}=0.9, and the second for a_{th}=0.4 and p_{pl}=0.8. A second type of POD curve which will be considered is only slightly more sophisticated, showing a sloped transition between p=0 and $p=p_{pl}$ (and thus requiring for complete definition a third parameter, a_{pl}, i.e. the crack depth at which $p=p_{pl}$ is attained). Figure 3 also includes one example of such a curve (a_{th}=0.6, a_{pl}=0.7 and p_{pl}=0.7). This latter type of curve will be used to investigate the value added by having a slightly more informative POD curve.

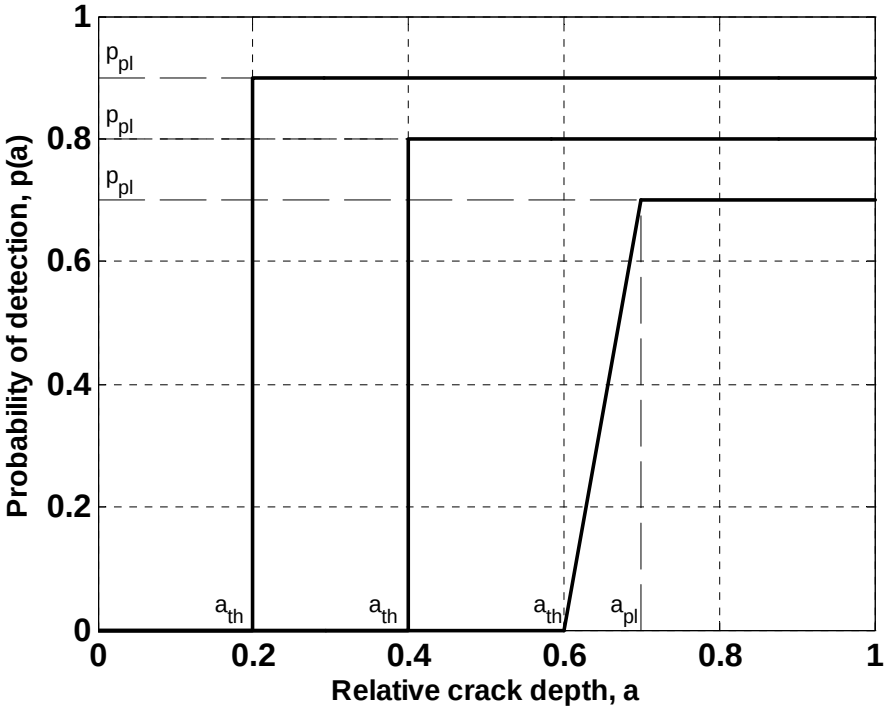

Figure 3 User-defined probability-of-detection curves

4 Base cases

We start by exploring some base cases. In each case, the risk reduction, *R*, obtained from Equation 2 will be calculated and plotted for several combinations of user-defined POD curves. Considering the generic POD step function of Figure 3, defined by the pair (a_{th}, p_{pl}), a_{th} will be explored over its complete range [0, 1], whereas six discrete values (1, 0.975, 0.95, 0.9, 0.85, 0.80) will be considered for p_{pl}. These are all cases with a sharp step, with no transitional region.

The different cases analysed are described below, and for each the results (in terms of risk reduction) are reported. The cases are summarised in Table 1, and described more in detail below.

Table 1 Summary of base cases

Probability of failure, $\phi(a)$	Flaw depth distribution, $\lambda(a)$		
	μ=0.01	μ=0.1	μ=10
	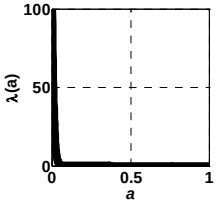	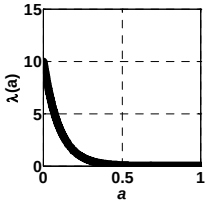	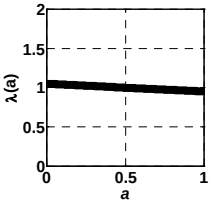
α=1, β=1 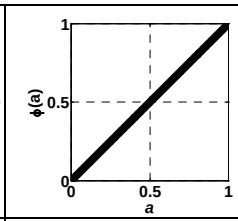	CASE 1a	CASE 1b	CASE 1c
α=10, β=100 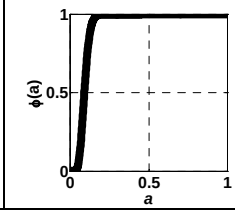	CASE 2a	CASE 2b	CASE 2c
α=100, β=10 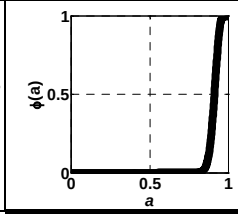	CASE 3a	CASE 3b	CASE 3c

CASE 1: Linear relationship between probability of failure and flaw size

In this case, the probability of failure varies linearly with flaw size between 0 and 1. In other words, using Equation 9 with parameters α=1, β=1:

$$\phi(x) = F(x;1,1) = x \tag{11}$$

We model $\lambda(\alpha)$ using a truncated exponential distribution as expressed in Equation 5, and consider three different cases for the parameter μ (0.01, 0.1 and 10), corresponding to three different expected values (0.01, 0.0999, 0.492). In the first 2 cases (μ=0.01, μ=0.1), the truncated exponential distribution virtually coincides with the non-truncated exponential. The third case is considered to represent a crack size distribution which is virtually uniform, and represents the situation of $\mu \to \infty$ (the distribution is virtually uniform for μ=10, and further increments of μ do not change its shape), see Figure 1.

CASE 2: Probability of failure showing a sharp increase at *a*=0.1

Here we consider a case in which the relationship between probability of failure and flaw size presents a rather sharp increase from zero to one, occurring approximately at *a*=0.1. This is obtained from Equation 9 using the parameters α=10 and β=100, see Figure 2. Again, we model $\lambda(\alpha)$ using a truncated exponential distribution as expressed in Equation 5, and consider three different cases for the parameter μ (0.01, 0.1 and 10).

CASE 3: Probability of failure showing a sharp increase at *a*=0.9

Here we consider a case in which the relationship between probability of failure and flaw size presents a rather sharp increase from zero to one, occurring approximately at *a*=0.9. This is obtained from Equation 9 using the parameters α=100 and β=10, see Figure 2.

The figures in the following pages show the risk reduction obtained in these 9 cases, for the different POD curves considered.

4.1 CASE 1a: μ=0.01, α=1, β=1

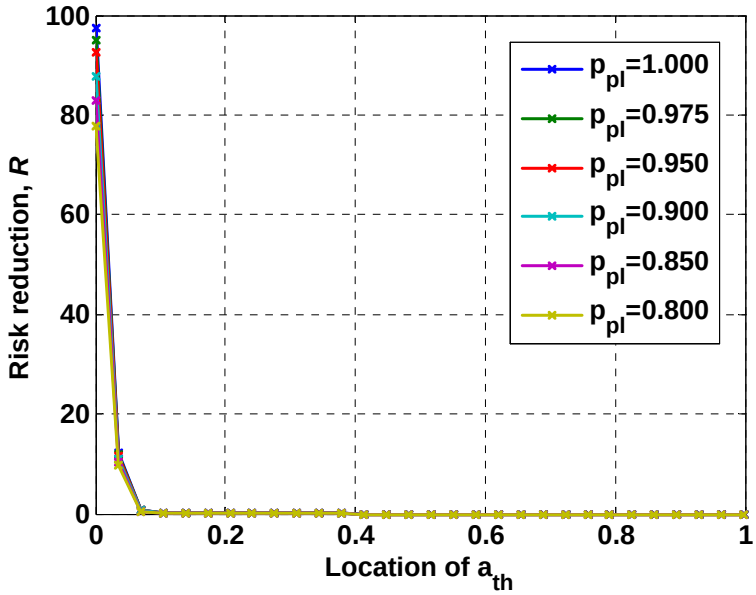

Figure 4 Risk reduction for case 1a and different sets of POD curves

4.2 CASE 1b: μ=0.1, α=1, β=1

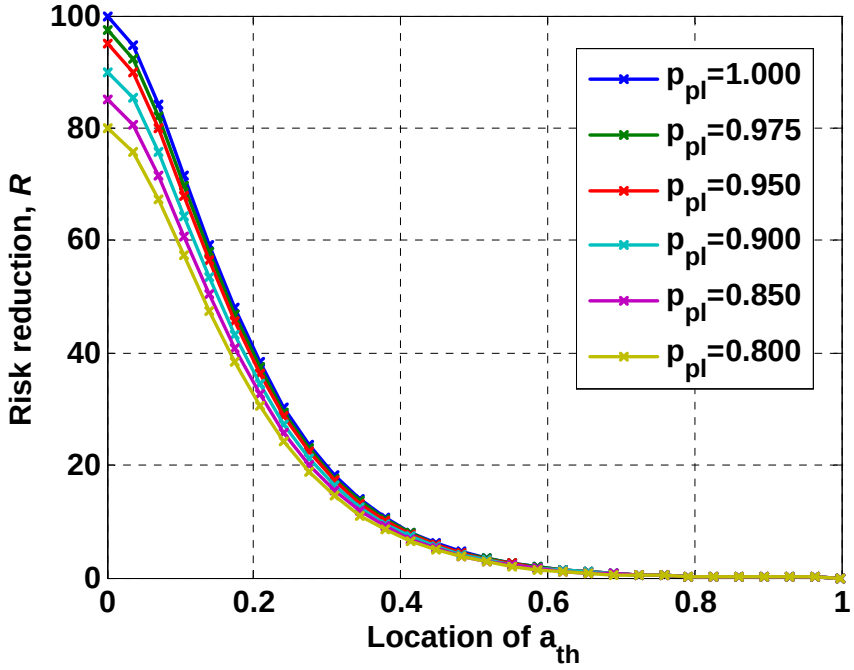

Figure 5 Risk reduction for case 1b and different sets of POD curves

4.3 CASE 1c: μ=10, α=1, β=1

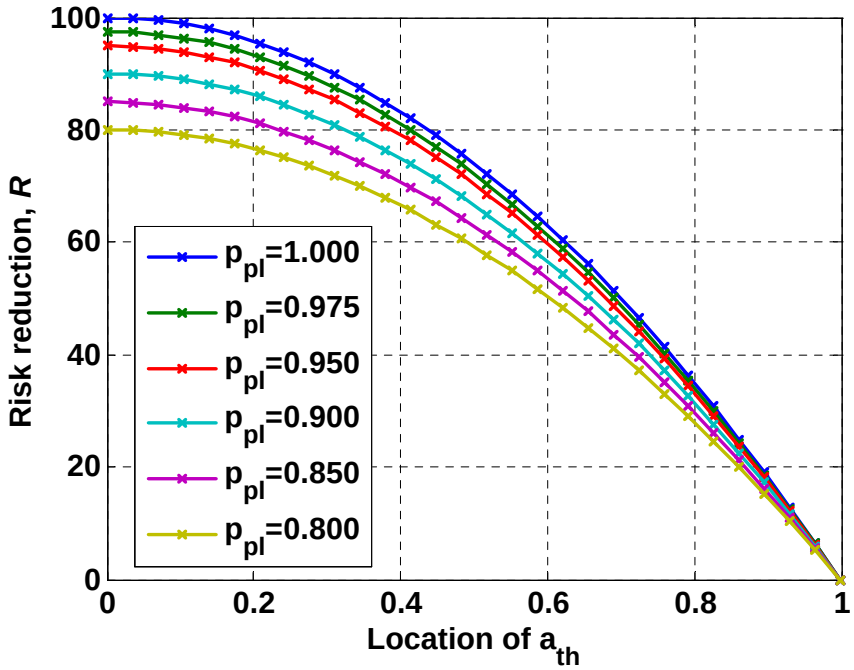

Figure 6 Risk reduction for case 1c and different sets of POD curves

4.4 CASE 2a: μ=0.01, α=10, β=100

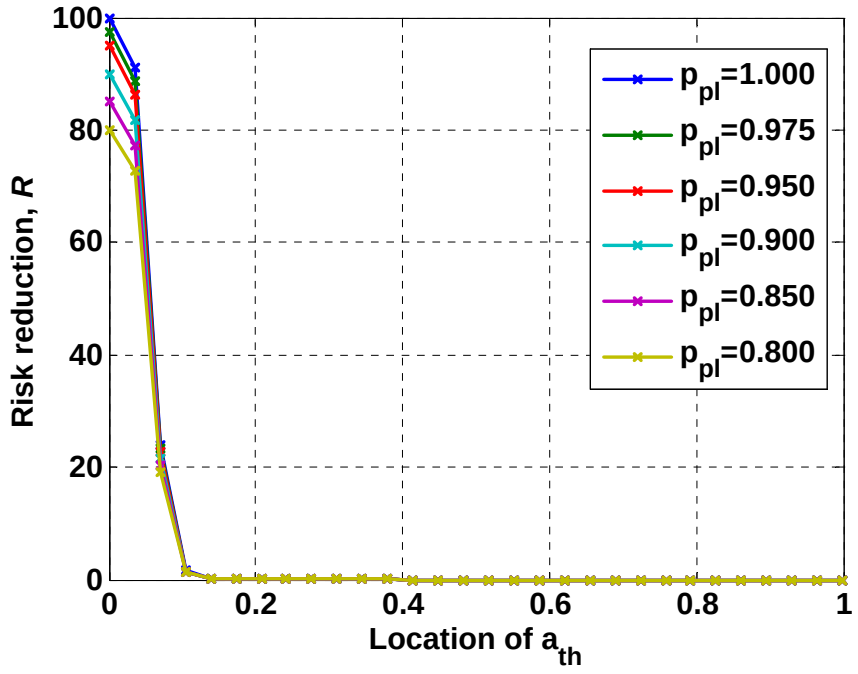

Figure 7 Risk reduction for case 2a and different sets of POD curves

4.5 CASE 2b: μ=0.1, α=10, β=100

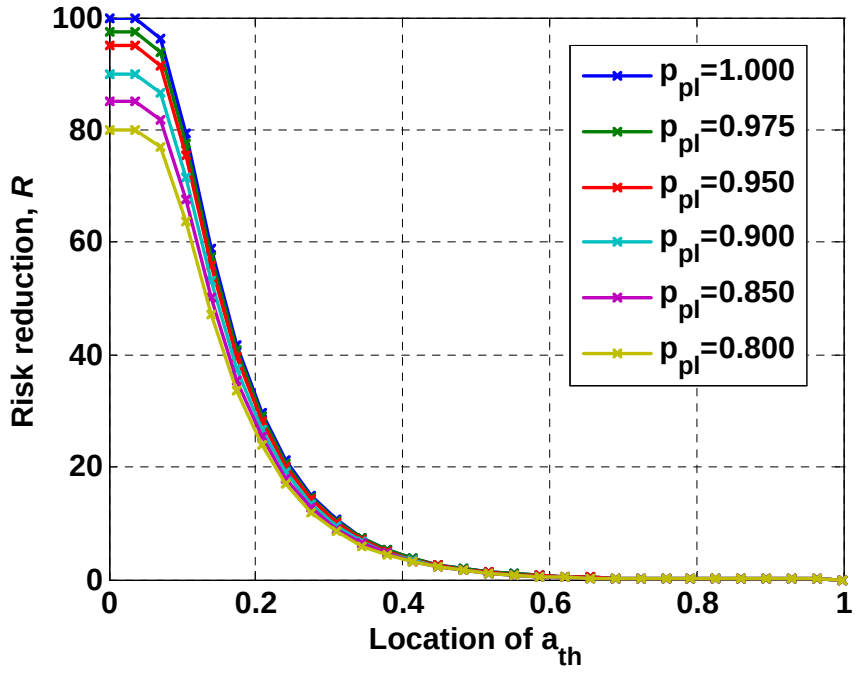

Figure 8 Risk reduction for case 2b and different sets of POD curves

4.6 CASE 2c: μ=10, α=10, β=100

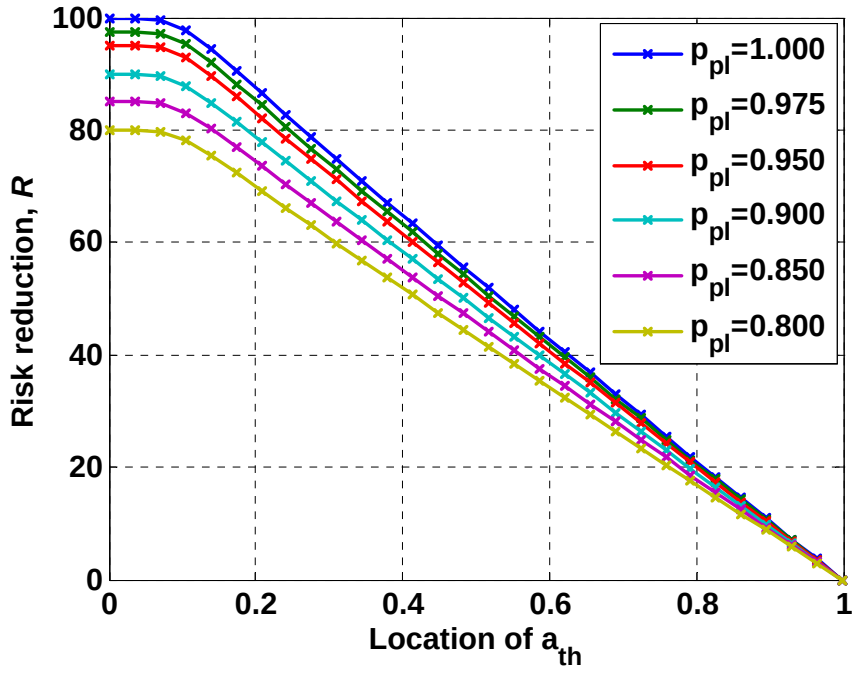

Figure 9 Risk reduction for case 2c and different sets of POD curves

4.7 CASE 3a: μ=0.01, α=100, β=10

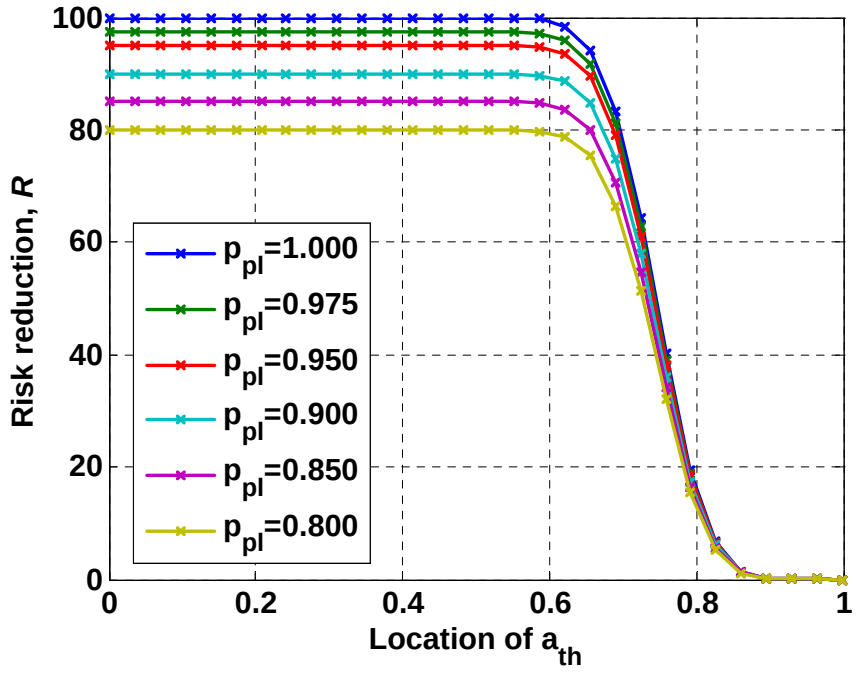

Figure 10 Risk reduction for case 3a and different sets of POD curves

4.8 CASE 3b: μ=0.1, α=100, β=10

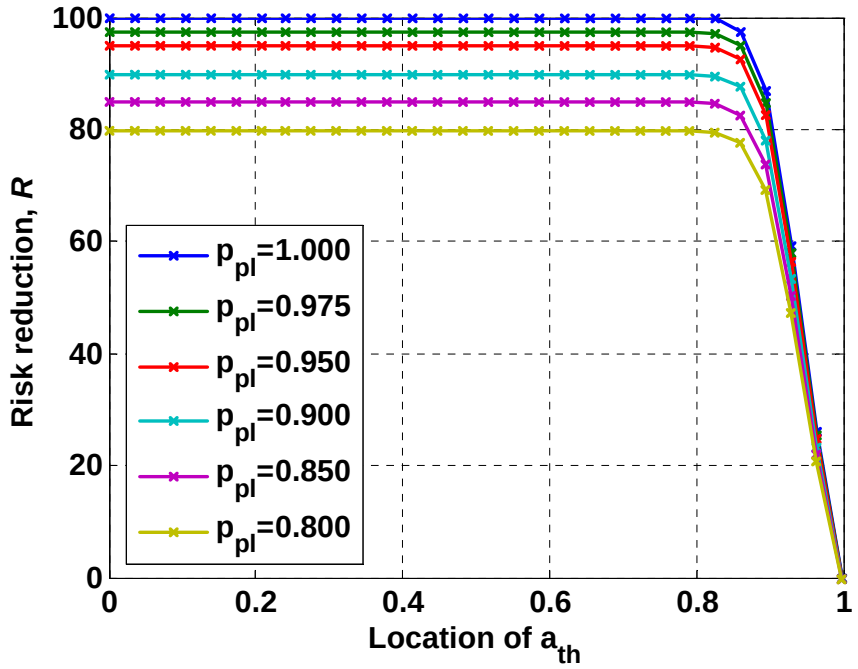

Figure 11 Risk reduction for case 3b and different sets of POD curves

4.9 CASE 3c: μ=10, α=100, β=10

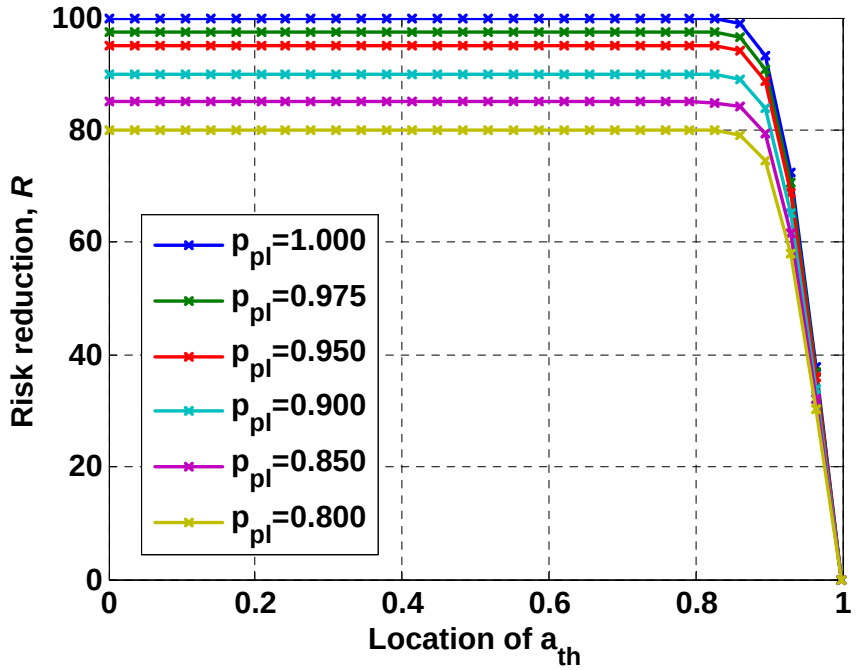

Figure 12 Risk reduction for case 3c and different sets of POD curves

4.10 Discussion

We start this discussion by recalling that the risk reduction, as defined in Equation (2), expresses a percentage change from a value of risk with no inspection to a value with inspection. Therefore, *R* takes values in the interval (0,100). When *R* is close to 100 a significant risk reduction due to the inspection has been achieved. When *R* approaches zero, a small change in risk has taken place.

It is clear that the information carried by *R* allows for a direct comparison between the probability of failure (and hence the risk) of a single component with and without the completion of an inspection. This is the goal of this study, and for this reason *R* has been so defined, but it is of some interest to consider briefly the significance of the absolute values of probability of failure (before doing any inspection) involved when moving from one situation (described by a pair of functions [λ(a), ϕ(a]) to another.

In Figure 13, the probability of failure, calculated for the three different functions $\phi(a)$ used in the basic cases above, is plotted against the varying expected value, μ', of the truncated exponential distribution chosen to represent the crack depth probability density. The parameter μ' varies between 0 and 0.5 (when the truncated exponential becomes coincident with the uniform distribution). It is worth recalling that μ is the mean of the underlying un-truncated exponential distribution and μ' is the mean of the truncated exponential distribution, given by Equation (6).

It is clear that, especially for those cases when μ' is small (which should represent real crack depth distributions), the absolute values obtained can vary by several order of magnitude from one situation to another. For instance, for μ' = 0.05, the probability of failure of a situation described by a function $\phi(a)$ presenting a rapid 0-to-1 transition at approximately a=0.1 (red line in Figure 13, typical of a crack in a brittle material) is 10^7 times higher than that of a function $\phi(a)$ presenting a similar transition at approximately a=0.9 (blue line, typical of a crack in a tough material).

Thus, a reduction of say R=50% in the risk obtained inspecting a component representative of the former situation would be much more valuable than a R=50% reduction in the risk obtained inspecting a component representative of the latter. These considerations are of course the very foundation of risk-informed inspection optimisation. As stated, we are here only considering the analysis of the relative effect of an inspection system on a single component.

CASE 1 (Probability of failure varying linearly with crack size)

Figure 4 shows that if the crack depth probability distribution has a small expected value (μ=0.01, implying that the near totality of the probability mass is approximately below 4% of wall thickness), only an inspection characterised by a POD curve with an a_{th} below 0.05 will be able to make any difference at all. Below this value, further reductions of a_{th} will have a great effect.

Figure 5 and Figure 6 show that, as the expected value of the crack depth probability distribution increases, the location of the POD curve step becomes more important even at higher values. The level of the POD plateau, p_{pl}, also becomes important.

It is interesting to note that curves such as those plotted in these figures could be used to make a choice on how the resources allocated to the design and qualification of an inspection system could be invested. Different strategies could be envisaged:

- For a given, fixed a_{th}, (which could be seen as the qualification size in the ENIQ methodology [8]), determine which level p_{pl} should be used to obtain the desired risk reduction;

- For a given, fixed p_{pl}, determine which a_{th} should be used to obtain the desired risk reduction;

- A combination of the two above, maximising the risk reduction for the given resources (it could be the case that it is much easier – and cheaper – to push down a_{th} rather than push up p_{pl}, and still obtain the same risk reduction.

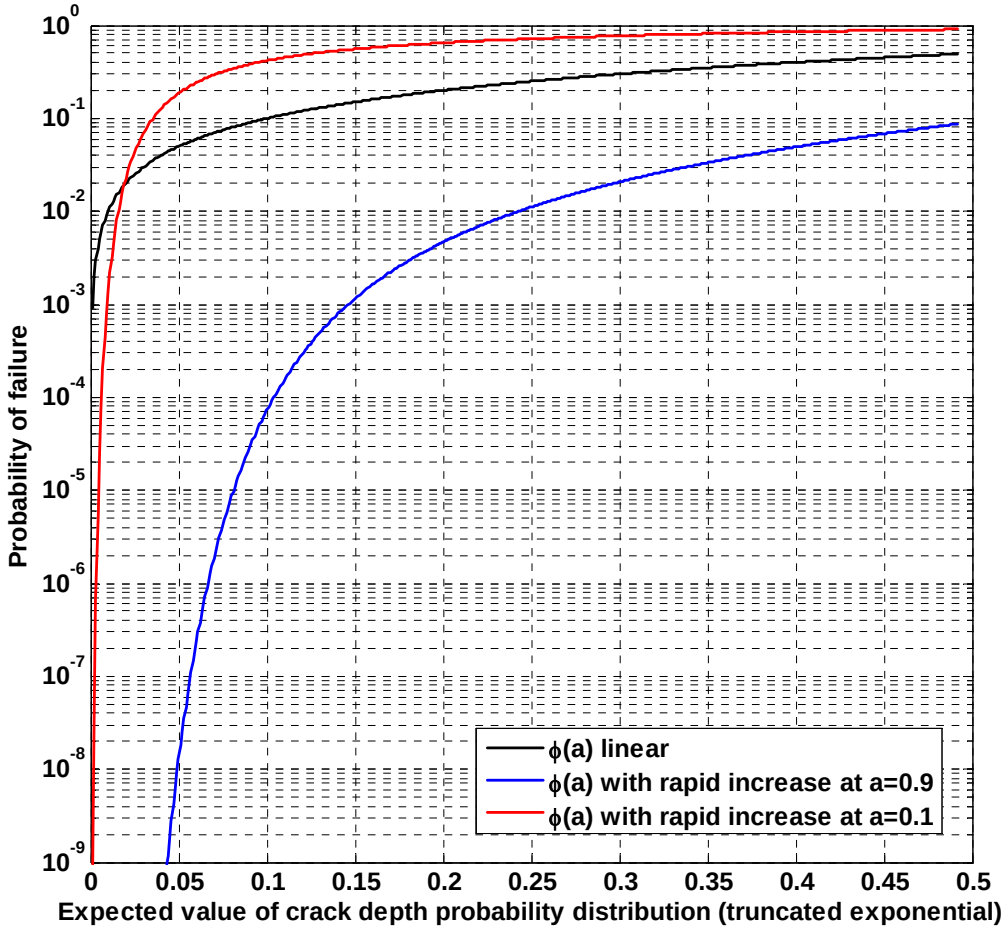

Figure 13 **Probability of failure calculated for different functions ϕ(a), plotted against a varying expected value, μ', of the truncated exponential distribution chosen to represent the crack depth probability density**

CASE 2 (Probability of failure increases rapidly around a = 0.1)

In the second case, the probability of failure was assumed to increase rapidly for rather shallow cracks (a ≅ 0.1). In Case 2a (Figure 7), a_{th} should be rather small to obtain any risk reduction, since the contribution of the cracks of the size just above the step in the failure probability function contribute the most to the failure probability. When the crack size distribution is assumed uniform, the risk reduction becomes linearly dependent of the location of a_{th}, except for the small values below and around the step in the failure probability function.

One should keep in mind that the failure probability function assumed for Case 2 is realistic mainly for very brittle materials, and such behaviour is not expected in normal piping systems.

CASE 3 (Probability of failure increases rapidly around a = 0.9)

Figures 10-12 show the results for the case where the probability of failure is nearly zero until a sharp increase when the crack depth is about 90% of the wall thickness. In all the analysed cases, independent of the assumption made on the initial crack depth distribution, the risk reduction is independent of the location of a_{th} up to at least a_{th}=0.6. The figures differ from each other only for large values of a_{th}. The reason why in Case 3a the drop in risk reduction occurs earlier can be explained by the fact that the probability of deep initial cracks is practically zero, and thus there is practically no risk that could be reduced.

The interesting conclusion that may be drawn from Case 3, is that as long as the a_{th} is within reasonable limits (and in practice detection threshold requirements are usually set much lower than half of the wall thickness), its exact value has no practical importance. The risk reduction is the same as if one had assumed a constant POD value equal to the plateau value p_{pl}. If the probability of failure function is modified to correspond to the one in Figure 23 based on a fracture mechanistic calculation, the sensitivity analysis results would still lead to similar conclusions for a realistic range of the a_{th}.

5 Adding information to the POD curve

In this section, we investigate the effects of adding “information” to the POD curves used in the analysis. In other words, we want to see the effect on the risk reduction introduced by POD curves which are more than a simple step function occurring at some crack depth a_{th}. With reference to Figure 3, we now consider POD curves defined by three parameters: a_{th}, a_{pl} and p_{pl}.

Let us define the following quantity, a_{av}, average crack depth of a_{th} and a_{pl}:

$$a_{av} = (a_{th}+a_{pl})/2 \qquad (12)$$

We can imagine a family of POD curves that, given a plateau value p_{pl}, are characterised by a constant value a_{av}, see Figure 14. For any given a_{av}, the probability of detecting a defect whose depth is a uniformly distributed random variable would be exactly the same for all curves in the family. Now we are interested to study the effect of the slope in the

POD function on the risk reduction with the previously defined different assumptions concerning the flaw size distribution and the probability of failure as a function of flaw size. If we are in a situation where all POD curves of one family are equivalently expensive in terms of resources needed to obtain them, it becomes of interest to investigate how the risk reduction varies from one member to the family to another. In this way, it is possible to determine the optimal member of the family as the curve maximising the risk reduction in the situation at hand.

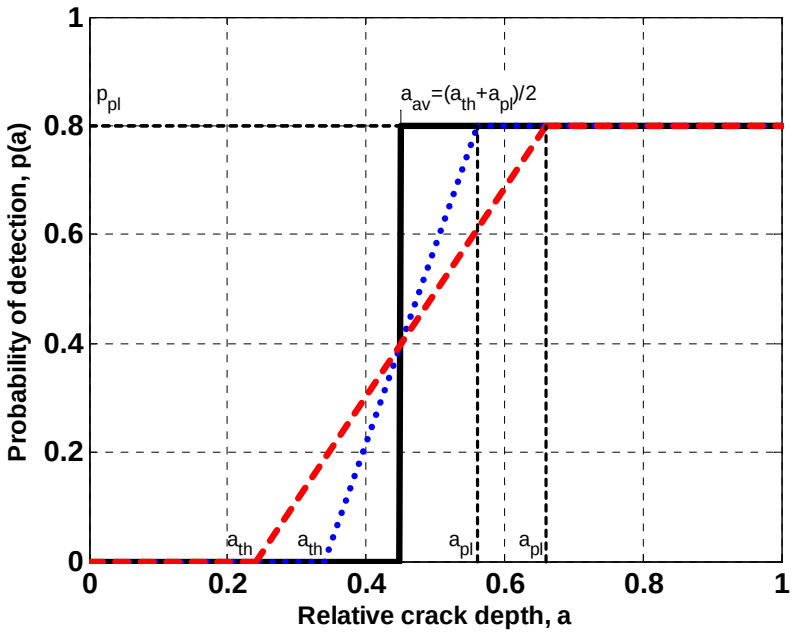

Figure 14 POD curves characterised by constant a_{av}.

In the following, we have applied this idea to base cases 1b, 2b and 3b. For clarity, only two plateau levels have been included (p_{pl}=0.8 and p_{pl}=1). Three families have then been considered, characterised by a_{av}=0.25, 0.5 and 0.75. The calculated risk reduction is plotted in Figure 15, Figure 16 and Figure 17 versus the location of a_{th}. For instance, in Figure 15, for a_{av}=0.25 (black lines), when a_{th}=0.25, then a_{pl}=0.25 as well, and we fall back to base case 1b. When a_{th}=0, a_{pl}=0.5 and the risk reduction is greater.

The way the POD curve families are defined, and considering that a_{th} cannot be less than 0 nor a_{pl} more than 1, explains the ranges of the curves plotted in these figures. When a_{av}=0.75, a_{th} can take values only between 0.5 and 0.75 as a_{pl} is limited to values between 0.75 and 1.

In cases 1b and 2b the risk reduction becomes somewhat bigger when the slope of the POD curve gets gentler. This is due to the fact that the inspection can then capture a higher portion of the small cracks which dominate the size distribution (so much that this dominates the result). In case 3b (except for the average at 0.25) the dominant factor is the loss of a part the detection efficiency for deeper cracks as the slope of the POD curve decreases, and thus R decreases. In the case of a_{av}=0.25, this does not play a part since the sloping part of the POD curve terminates at a=0.5 or before, and the probability of failure curve, $\phi(a)$, only increases at around a=0.8.

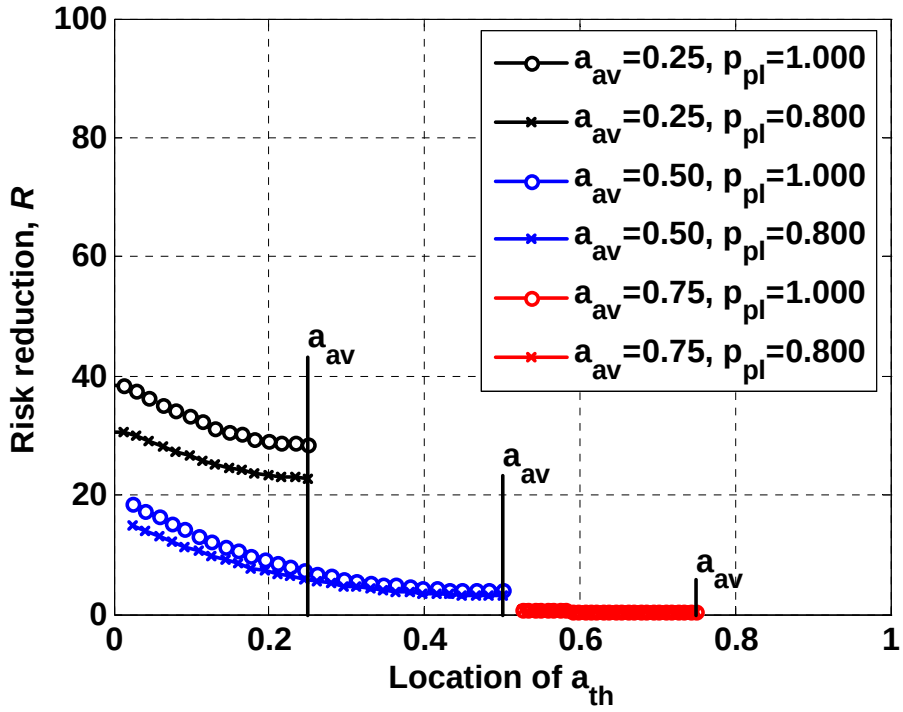

Figure 15 Risk reduction, *R*, obtained for different POD curves belonging to three families characterised by a_{av}=0.25, 0.5 and 0.75 (base case: 1b).

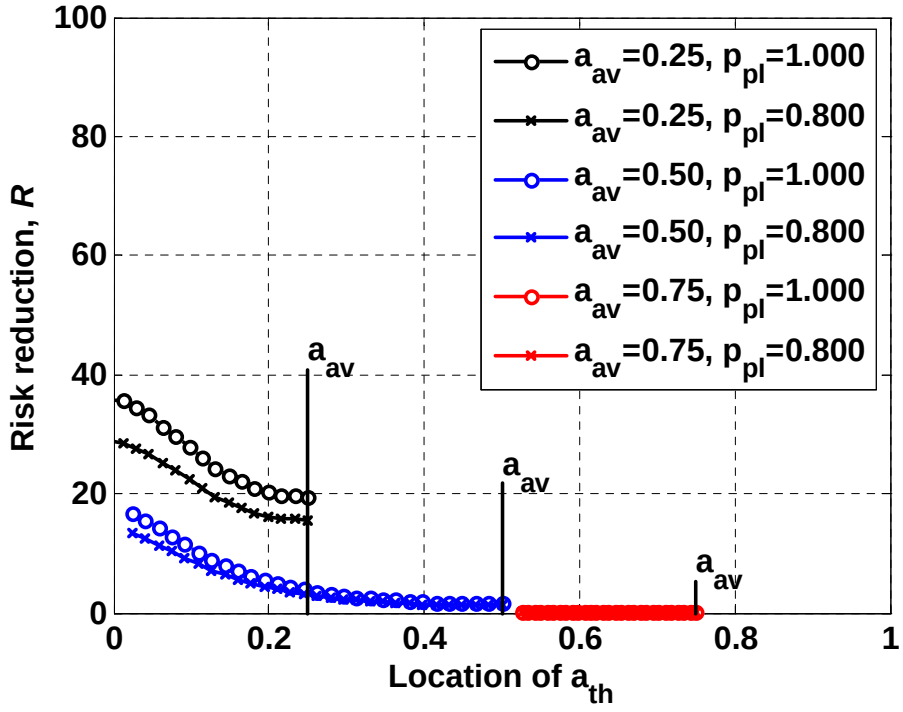

Figure 16 Risk reduction, *R*, obtained for different POD curves belonging to three families characterised by a_{av}=0.25, 0.5 and 0.75 (base case: 2b).

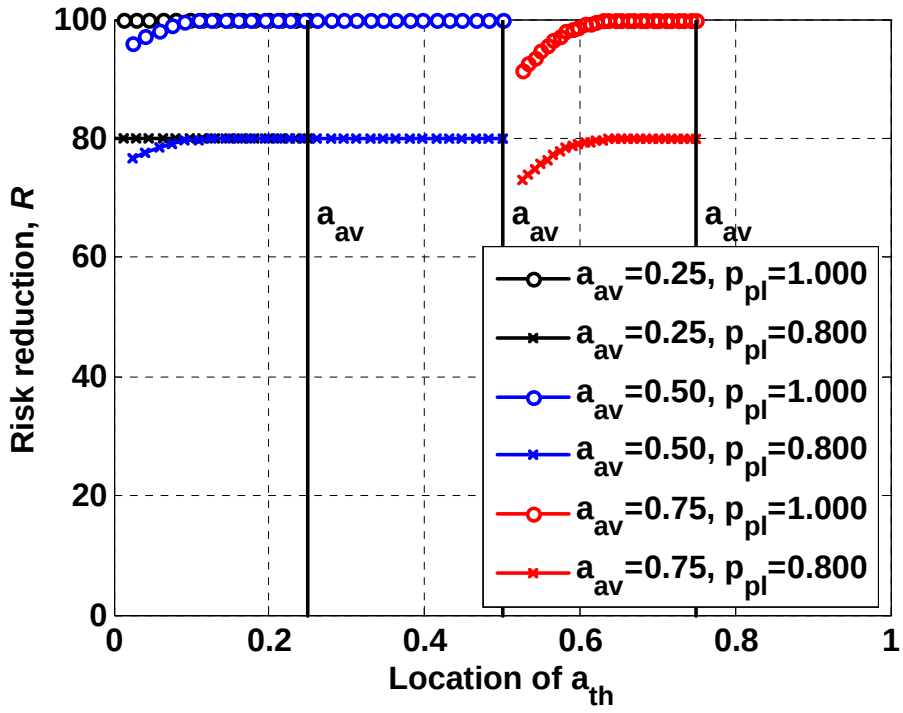

Figure 17 **Risk reduction, *R*, obtained for different POD curves belonging to three families characterised by a_{av}=0.25, 0.5 and 0.75 (base case: 3b).**

A second family of POD curves that can easily be investigated is illustrated in Figure 18. These POD curves are characterised by a constant value a_{pl}.

We applied this idea to base cases 1b, 2b and 3b. Again in the interest of clarity, only two plateau levels have been included (p_{pl}=0.8 and p_{pl}=1). Three families have then been considered, characterised by a_{av}=0.25, 0.5 and 0.75. The calculated risk reduction is plotted in Figure 19, Figure 20 and Figure 21 versus the location of a_{th}.

In case 3b, for instance, where the transition of the function $\phi(a)$ occurs at a=0.9, there is absolutely no added value in "adding" the sloping part of the curve to any of the considered step functions.

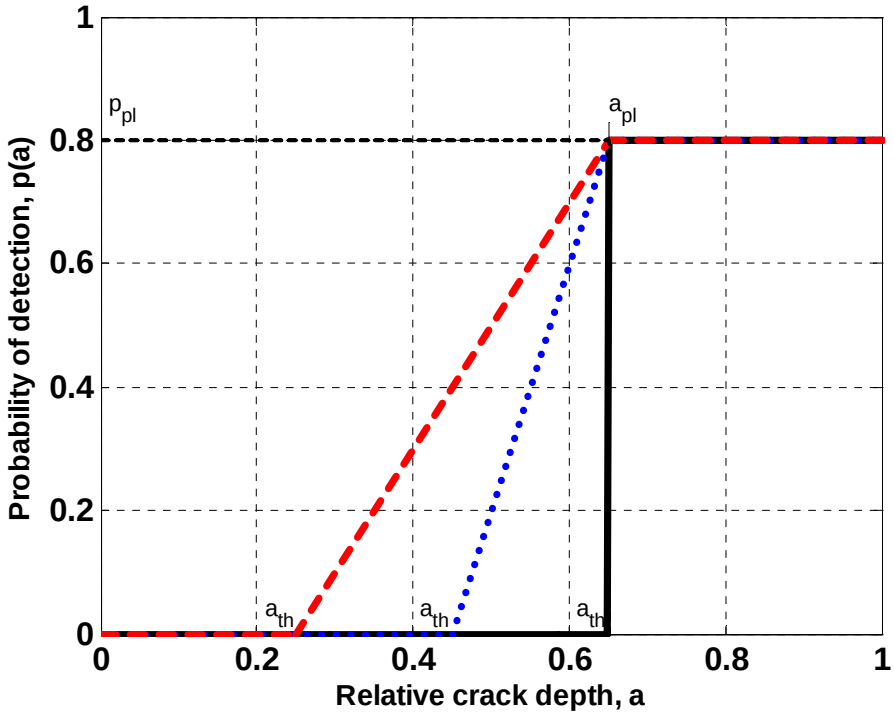

Figure 18 **POD curves characterised by constant a_{pl}.**

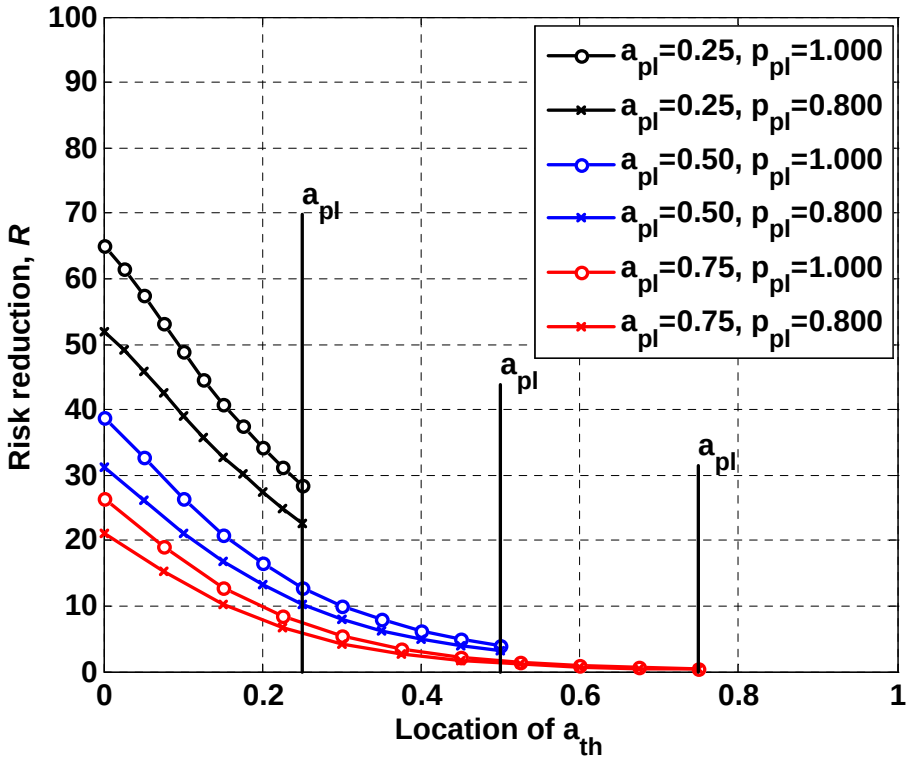

Figure 19 **Risk reduction, *R*, obtained for different POD curves belonging to three families characterised by fixed a_{pl}=0.25, 0.5 and 0.75 (base case: 1b).**

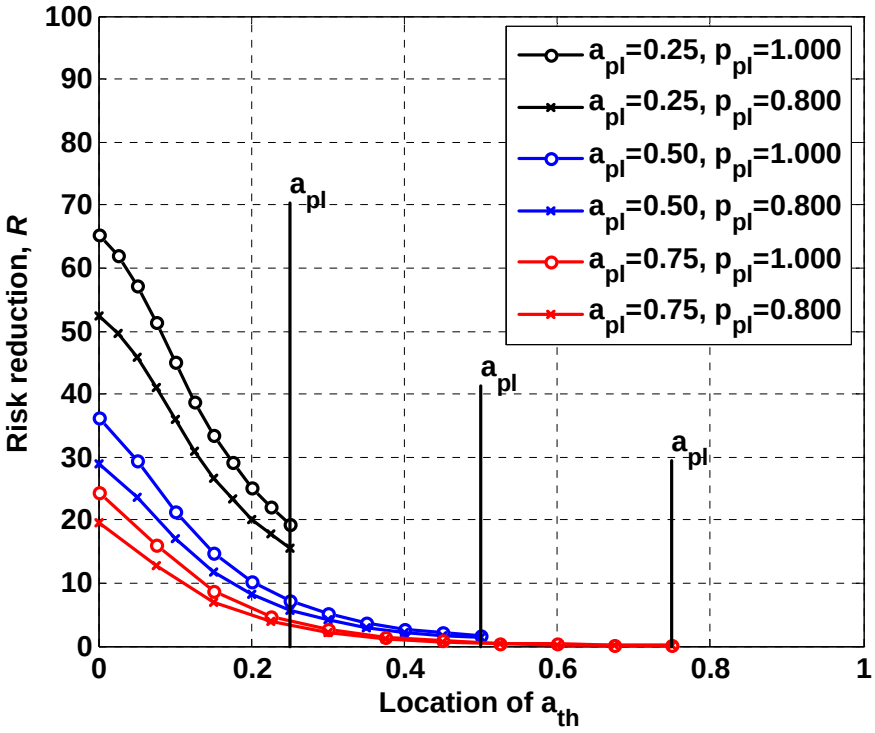

Figure 20 **Risk reduction, *R*, obtained for different POD curves belonging to three families characterised by fixed a_{pl}=0.25, 0.5 and 0.75 (base case: 2b).**

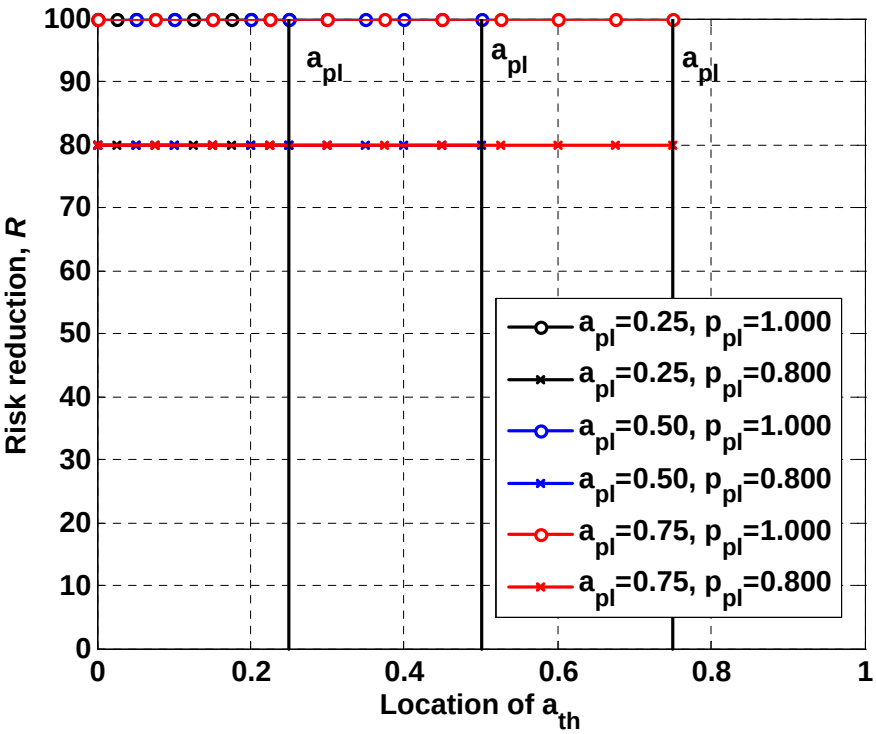

Figure 21 **Risk reduction, *R*, obtained for different POD curves belonging to three families characterised by fixed a_{pl}=0.25, 0.5 and 0.75 (base case: 3b).**

6 Conclusions

In this document we have discussed the link between risk-informed in-service inspection (RI-ISI) and assumptions made concerning the probability of flaw detection. The purpose was to investigate which practical requirements should be set for assumptions about the accuracy of probability of detection (POD) curves from a RI-ISI point of view.

We have proposed a simplified approach that allowed us to avoid making detailed assumptions about the relationship between crack size and probability of failure, the probability distribution of crack size and the shape of the POD curve. The determination of the two functions describing (1) failure probability as a function of flaw size and (2) flaw distribution would be in a real situation relatively resource-consuming exercises. The examples presented herein include both realistic cases and more extreme situations, helping to analysis the sensitivity of risk-reduction through inspections.

The cases that most closely model a real situation are those where the expected value of the defect distribution is not greater than 0.1 (one tenth of wall thickness), and the probability of failure is very low unless the flaw depth is significant. The toughness of metals used in the nuclear industry would tend to exclude situations where the probability of failure would be high with very shallow cracks. In the realistic situations, the location of a_{th} plays a rather insignificant role, unless it is unrealistically high (e.g. more than 70-80%,) and the risk reduction is controlled by the value of p_{pl}.

We do not draw more detailed conclusions regarding the examples at hand because the purpose of this report is rather to suggest a method for analysis. Each user can straightforwardly draw his or her own conclusions according to the input functions used.

In the present study, crack growth or other time-dependent phenomena have not been considered. The effect of time is twofold. First, the flaw size distribution would evolve (flaws would initiate, other would grow to become fully penetrating, etc.). Second, the material properties would change, affecting the shape of the function $\phi(a)$, i.e. the probability of failure as a function of flaw size (see example in Appendix 1).

The most important shortcoming of excluding time-related effects in the analysis is that we cannot presently investigate the effect of inspection intervals on risk-reduction. Future work will involve extending the sensitivity analyses to take into account crack growth, which will allow us to study various inspection strategies. One possible approach for such investigations is the use of Markov models. Applications of continuous-time Markov processes have been presented by Fleming [9], and discrete-time Markov chain studies of inspection strategies have been reported by Cronvall et al. [10]. In the latter approach, probabilistic fracture mechanics calculations are integrated with a discrete-time Markov process analysis to model piping degradation states at inspections, and accounting for flaw and leak detection probabilities. This approach seems suitable for our purposes as well.

7 Acknowledgements

The authors wish to acknowledge Dr. B. Shepherd of Doosan Babcock, Dr. R. Chapman of British Energy and S. Olsson of OKG for their valuable comments.

8 References

[1] U.S. Nuclear Regulatory Commission: Regulatory Guide 1.174 - An Approach for Using Probabilistic Risk Assessment in Risk-Informed Decisions on Plant-Specific Changes to the Licensing Basis. Rev. 1 (2002).

[2] U.S. Nuclear Regulatory Commission: Regulatory Guide 1.178 - An Approach for Plant-Specific Risk-Informed Decisionmaking for Inservice Inspection of Piping. Rev. 1 (2003).

[3] Brickstad B, Zang W. NURBIT nuclear RBI analysis tool—a software for risk management of nuclear components. DNV Report 01334900-1, Sweden; 2001.

[4] Simonen FA, Woo, H.H., Analyses of the Impact of Inservice Inspection Using a Piping Reliability Model, NUREG/CR-3869, 1984.

[5] Simonen FA, Doctor SR, Dickson TL, Distributions of Fabrication Flaws in Reactor Pressure Vessels for Structural Integrity Evaluations, ASME Pressure Vessels and Piping Conference, Vancouver, Canada (2002).

[6] Nilsson KF, Blagoeva D, Moretto P, An experimental and numerical analysis to correlate variation in ductility to defects and microstructure in ductile cast iron components, Engineering Fracture Mechanics 73 (2006) 1133–1157

[7] Berens, AP, NDE reliability data analysis. In Metals Handbook, 9th edn, Vol. 17, ASM Int., 1989, pp. 689-701.

[8] European methodology for qualification of non-destructive testing: second issue. EUR 17299 EN. 1997.

[9] Fleming, K.N. Markov models for evaluating risk-informed in-service inspection strategies for nuclear power plant piping systems, Reliability Engineering & System Safety, Volume 83, Issue 1, January 2004, Pp. 27-45.

[10] Cronvall, Otso; Männistö, Ilkka; Simola, Kaisa. Development and testing of VTT approach to risk-informed in-service inspection methodology. Final report of SAFIR INTELI INPUT Project RI-ISI. 2007. VTT, Espoo. 43 p. VTT Research Notes 2382. http://www.vtt.fi/inf/pdf/tiedotteet/2007/T2382.pdf

Appendix 1 - EXAMPLE

Probability of failure of cylinder under constant tension

Let us consider a cylinder with an outer radius of 1m and an inner radius of 0.9m, subject to a constant uniform axial tension, σ_T, of 200 MPa. Let us assume the presence of a semi-elliptical inner surface-breaking crack, of depth *a* and length *2c*. Let us assume that the material initiation toughness, K_{IC}, is a normally distributed random variable, with mean μ_{KIC} equal to 150 MPa$\sqrt{m}$ and standard deviation σ_{KIC} equal to 20 MPa$\sqrt{m}$. Let us also assume that 2*c*=10*a*.

With reference to Figure 22, the stress intensity solution at the deepest point of the crack, K_I, is given in [A1] as:

$$K_I(a) = \sigma_T \sqrt{\frac{\pi \cdot a}{Q}} F_t \tag{A1}$$

where

$$F_t = 1 + [0.02 + \xi(0.0103 + 0.006175\xi) + 0.0035(1 + 0.7\xi)\left(\frac{R_i + R_o}{2t}\right)^{0.7}] \cdot Q^2$$
$$\xi = \frac{2c}{t} \qquad Q = 1 + 1.464\left(\frac{a}{c}\right)^{1.65} \tag{A2}$$

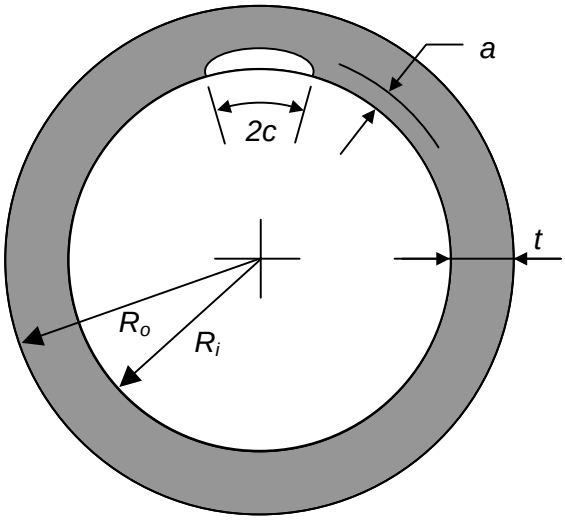

Figure 22 Cylinder with semi-elliptical inner surface-breaking crack

Let us assume the following failure criterion:

$$K_I > K_{IC} \tag{A3}$$

In other words, we assume that the component has failed if the stress intensity factor at the crack tip exceeds the material initiation toughness.

Under this assumption, the probability of failure, $\varphi(a)$, for a crack of size *a* can be easily obtained as:

$$\varphi(a) = \Phi\left(\frac{K_I(a) - \mu_{KIC}}{\sigma_{KIC}}\right) \tag{A4}$$

where $\Phi(x)$ is the standard normal cumulative distribution function.

Equation (A4) is plotted in Figure 23 using the numerical data of the example. It is clear to see that the cumulative Beta distribution functions shown in Figure 2 are well suited to represent this type of behaviour.

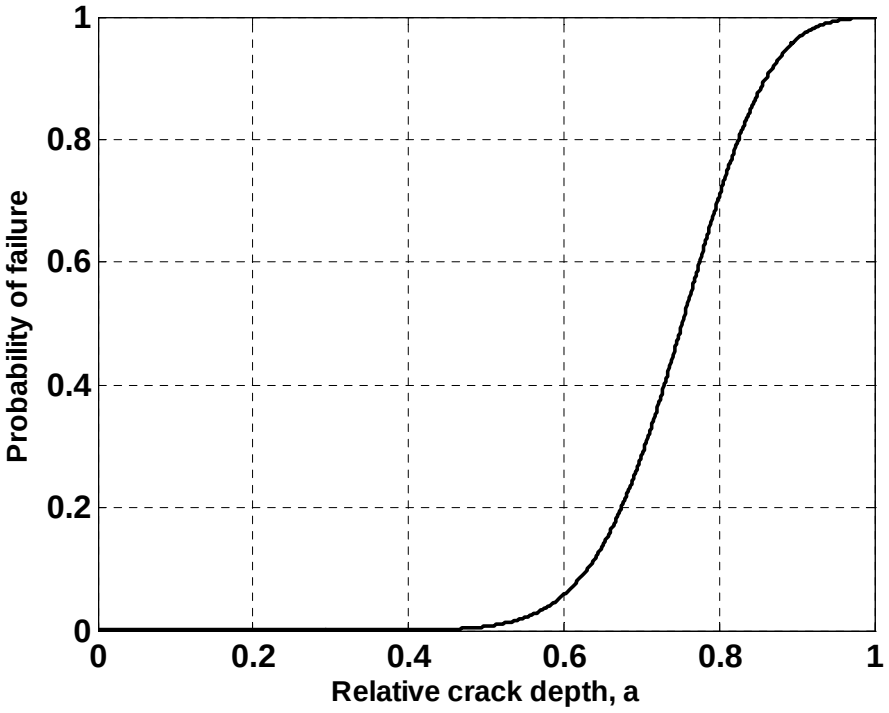

Figure 23 Failure of probability versus crack size, $\varphi(a)$, for crack in cylinder under constant tension

Let us now suppose that the material of the component is subject to some aging-related embrittlement. We model this by assuming that every year μ_{KIC} is reduced by 5%, and that σ_{KIC} is reduced by 2%. In this way, σ_{KIC} becomes bigger relative to μ_{KIC}. These values are purely illustrative.

Equation (A4) can be used again to obtain new probability of failure curves as functions of crack depth, for any subsequent year starting from today (Figure 24). Again, the cumulative Beta distribution functions shown in Figure 2 are well suited to represent this type of behaviour.

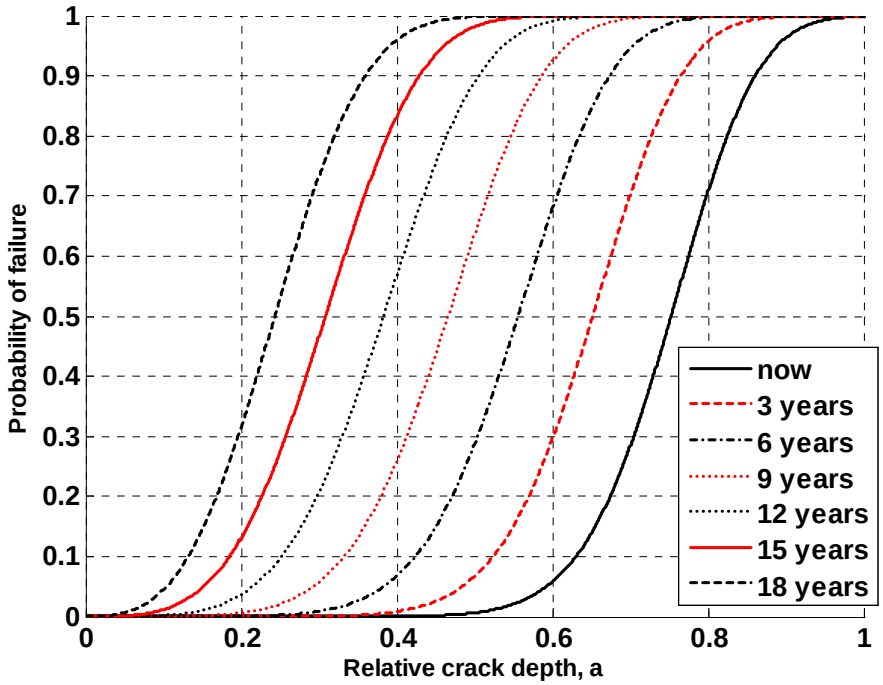

Figure 24 **Failure of probability versus crack size curves (for crack in cylinder under constant tension), obtained assuming a progressive material embrittlement.**

References

[A1] T.L. Anderson, Fracture Mechanics – Fundamentals and applications, 2nd edition, CRC Press.

European Commission

EUR 21902 EN – DG JRC – Institute for Energy
SENSITIVITY OF RISK REDUCTION TO PROBABILITY OF DETECTION CURVES (POD) LEVEL AND DETAIL

Authors
Luca Gandossi DG-JRC-IE
Kaisa Simola VTT Technical Research Centre of Finland

Luxembourg: Office for Official Publications of the European Communities
2007 – 22 pp. – 21 x 29.7 cm
EUR - Scientific and Technical Research Series; ISSN 1018-5593

Abstract
This report discusses the link between risk-informed in-service inspection (RI-ISI) and assumptions made concerning the probability of flaw detection. The purpose is to investigate the reasonable and practical requirements that should be set for assumptions about the accuracy of probability of detection (POD) curves from a RI-ISI point of view.

The mission of the Joint Research Centre is to provide customer-driven scientific and technical support for the conception, development, implementation and monitoring of EU policies. As a service of the European Commission, the JRC functions as a reference centre of science and technology for the Union. Close to the policy-making process, it serves the common interest of the Member States, while being independent of special interests, whether private or national.